Characterisation of Notch1-mediated transcription in cortical pyramidal neurons reveals a negative feedback mechanism involving HDAC4

3

Martijn Dahlhaus, Willem Kamphuis, Joop M. van Helvoort, Marian J. Groot Koerkamp, Frank C. P. Holstege and Christiaan N. Levelt

PLoS One under revision

Abstract

Notch1-signalling is a key pathway for various early developmental processes in the CNS. By now, it is clear that Notch1 also plays an important role in regulating migration, neurite outgrowth and structural- and functional plasticity in postmitotic neurons of the cerebral cortex. To determine the targets of Notch1-regulated transcription that may mediate these effects on plasticity, we performed microarray analyses in mice overexpressing constitutively active Notch1 in cortical pyramidal neurons. We found that in these animals Notch1 predominantly regulates genes involved in transcription and in signalling through the Ras/MAPK pathway. In addition, we identified a negative feedback loop involving the class II histone deacetylase HDAC4, restricting Notch1-mediated transcription. These findings provide new insights in the mechanisms through which Notch1 regulates synaptic plasticity and transcription of its target genes in the juvenile and adult cortex.

Introduction

Notch signalling constitutes an evolutionary conserved signalling pathway regulating a variety of cellular processes during development and postnatal life. This includes cell-fate decisions, differentiation, proliferation and apoptosis. In recent years, a role of Notch1-signalling in postmitotic neurons has started to be appreciated. Notch1-signalling has been implicated in limiting neurite outgrowth in the first weeks after birth [Sestan et al., 1999; Redmond et al., 2000] and in regulating synaptic plasticity in the hippocampus [Wang et al., 2004] and the developing visual cortex [Dahlhaus et al., 2008]. Moreover, Notch1 has been found to interact with amyloid precursor protein (APP) signalling [Berezovska et al., 2001; Roncarati et al., 2002; Lleo et al., 2003; Fischer et al., 2005] and its expression is increased in Alzheimer's Disease and other brain disorders, suggesting that Notch1 may be involved in neurodegeneration. Notch1 is a single-span transmembrane protein, functioning as a receptor. Its ligands (in mammals Delta and Jagged) are single-span transmembrane proteins as well, embedded in the plasma membrane of neighbouring cells. Upon ligand-receptor binding, the Notch1 intracellular domain (NICD) is cleaved off [de Strooper et al., 1999] and translocates to the nucleus where it binds C-promoter binding factor (CBF1) [Lu et al., 1996], a member of a transcriptional repressor complex that also includes the co-repressors SMRT, C-terminal binding protein (CtBP) [Oswald et al., 2005] and class I histone deacetylases (HDACs) among others [Kao et al., 1998; Bertos et al., 2001]. Binding of the NICD to CBF1 induces removal of transcriptional repressors and recruitment of transcriptional activators Mastermind and histone acetyl transferases (HATs), thus resulting in transcription of downstream targets. A principle transcriptional Notch1-target is Hes1, a basic helix-loop-helix (bHLH) protein [Jarriault et al., 1995]. Additional molecular and cellular effects of Notch1-signalling seem to depend on the cellular and environmental context [Bray, 2006].

In this study, we set out to shed light on the molecular effects of Notch1-signalling in postmitotic cortical pyramidal neurons. We have previously reported that in a transgenic mouse model overexpressing a constitutively active form of Notch1 in neocortical pyramidal neurons from the fourth postnatal week onwards, neuronal morphology and visual plasticity were altered [Dahlhaus et al., 2008]. Here we have performed microarray analysis in the same animal model with the aim to identify molecular targets of Notch1-signalling potentially involved in regulating synaptic plasticity and neuronal morphology. We found a small set of Notch1-regulated genes that were mostly involved in transcriptional regulation or signalling through the Ras/

MAPK-pathway. Also, we uncovered a feedback loop involving HDAC4 that limits Notch-mediated transcription.

Materials & Methods

DNA Constructs and Transgenic Mice

The transgenic mice used in this paper have been described before [Dahlhaus et al., 2008]. Briefly, Notch transgenic mice conditionally overexpress the Notch Intracellular Domain (NICD) in all pyramidal neurons of the neocortical extragranular layers. NICD acts as an active Notch mutant that does not require activation by ligand binding, resulting in constitutive signalling of the Notch pathway. This mouse model has been validated before [Dahlhaus et al., 2008]. All experiments involving mice were approved by the Ethical Committee on the use of experimental animals of the Royal Netherlands Academy of Arts and Sciences.

DNA vectors for transfection

Flag-tagged HDAC4 in pcDNA3.1 was obtained from Addgene (Addgene plasmid 13821), the GFP vector was obtained from Invitrogen (pEGFP-N3) and the TK promoter-Luciferase vector was obtained from Promega (pTK-RL). The Hes1-luciferase reporter construct has been described earlier [Fischer et al., 2005], as has the NICD construct [Dahlhaus et al., 2008].

RNA isolation

Cerebral cortex from ten week old mice was dissected, snap-frozen in liquid nitrogen and stored at -80°C until RNA isolation using Trizol (Invitrogen). RNA yield was quantified on a Nanodrop (Nanodrop; Thermo Scientific) and quality assessed using an Agilent Bioanalyser (Agilent). Only samples with RNA Integrity Numbers (RIN's) of at least 8.0 were included.

Sample preparation, hybridization and data analysis

RNA samples were isolated from the cerebral cortex of 9 NICD+Cre+ animals and 6 littermate controls (NICD+Cre-, NICD-Cre+ or NICD-Cre-) of 10 weeks old. Group samples were made for NICD+Cre+ animals and controls by pooling equal amounts of RNA from each mouse. Pooled RNA was labelled and hybridized to microarrays; eight microarrays were used in parallel. On four of these arrays, RNA from control

animals was labelled with Cy3 and RNA from NICD+Cre+ animals with Cy5, while on the remaining four arrays the dyes were swapped.
Microarrays used were Mouse 70-mer oligos (Operon, Mouse V2 AROS) spotted onto Corning UltraGAPS slides as described before [Raaben et al., 2007]. Arrays contained 35000 spots (32101 70-mer oligonucleotides and 2891 control spots). RNA amplifications, labelling and hybridizations were performed as described before [Roepman et al., 2005].
Hybridized slides were scanned on an Agilent scanner (G2565AA) at 100% laser power, 30% PMT. After data extraction using Imagene 7.5 (BioDiscovery), print tip Loess normalization was performed [Yang et al., 2002] on mean spot-intensities. Data was analyzed using ANOVA (R version 2.2.1/MAANOVA version 0.98-7; http://www.r-project.org/). In a fixed effect analysis, sample, array and dye effects were modelled. P-values were determined by a permutation F2-test, in which residuals were shuffled 5000 times globally. Genes with $p<0.05$ after Benjamini Hochberg correction were considered significantly changed.

Quantitative RT-PCR

RNA was obtained as described for microarray analysis. Beside the mice used for microarray experiments, an additional 13 mice were added to both the control and the transgenic group. RNA was not pooled and individual mice were processed as individual samples throughout the experiment. cDNA was synthesized using the SuperScript® III First-Strand cDNA Synthesis Kit (Invitrogen). Oligonucleotide primers were designed with Primer Express 2.0 software and purchased from Eurogentec or Biolegio.
qPCR reactions were run on 1/20 diluted cDNA for genes of interest and candidate reference genes. SYBR® Green technology was used on a 7300 Real-Time PCR System (Applied Biosystems). Using GeNorm software (http://medgen.ugent.be/~jvdesomp/genorm/) an optimal set of reference genes was chosen based on similar expression patterns across samples [Vandesompele et al., 2002]. A geometrical mean of the set was used to normalize results of the genes of interest. Statistical significance was determined using Student's t-test. One-tailed testing was used for confirmation of microarray data. A p-value of <0.05 was considered statistically significant. For NICD, Hes1, Riam, S100a6 and NED, 19 controls and 22 transgenics were used. For Rasgef1c, Phlda3, HDAC4, Rasd2, Accn1 and Wnt10a, 11 controls

and 14 transgenics were used. For all qPCR reactions on cerebellar samples, 8 controls and 8 transgenics were used.

Forward and reverse primer sequences for qPCR were as follows:

primer	sequence
ACTG1-forward (fw)	CATTGCTGACAGGATGCAGAA
ACTG1-reverse (rv)	ACATCTGCTGGAAGGTGGACA
EF1alpha-fw	AAGAAGATCGGCTACAACCCAG
EF1alpha-rv	TTACGCTCTACTTTCCAGCCCT
GAPDH-fw	ATGTGTCCGTCGTGGATCTGA
GAPDH-rv	ATGCCTGCTTCACCACCTTCT
G6PDX-fw	GTCCAGAATCTCATGGTGCTGA
G6PDX-rv	GCAATGTTGTCTCGATTCCAGA
HPRT-fw	GCAAACTTTGCTTTCCCTGG
HPRT-rv	TTCGAGAGGTCCTTTTCACCA
Polr2a-fw	TTTGCGCTGTGTCTGCTTCTT
Polr2a-rv	TGCCCCTTAGATTTGGCCA
rs27a-fw	GGCCAAGATCCAGGATAAGGA
rs27a-rv	CCATCTTCCAGCTGCTTACCA
TBP-fw	CACGGACAACTGCGTTGATTT
TBP-rv	GCCCAACTTCTGCACAACTCT
NICD-fw	CGTACTCCGTTACATGCAGCA
NICD-rv	AGGATCAGTGGAGTTGTGCCA
Hes1-fw	TCAACACGACACCGGACAAA
Hes1-rv	CCTTCGCCTCTTCTCCATGAT
RIAM-fw	TCTGCTGTGATGACGCAAGAA
RIAM-rv	ACCAACAGTCCCCAGGTTTGT
S100a6-fw	ACTCTGGCAAGGAAGGTGACA
S100a6-rv	TCAGCCTTGCAATTTCAGCA
Phlda3-fw	CGCCACATCTACTTCACGCTAG
Phlda3-rv	TTGAACTTGACCAGGCCCA
Rasgef1c-fw	CGAGCATCACCCATTACCTGT
Rasgef1c	CTCGCTTTCATAGGAAGCCAA
HDAC4-fw	CTACATGTCCCTGCACCGCTAT
HDAC4-rv	TGACATTGAAACCCACGCCT
Rasd2-fw	“ATATCCTGGACACCTCTGGCA”

primer	sequence
Rasd2-rv	CAGGCTGAACACCAGGATGAA
Accn1-fw	GCTGGAGATCATGCTGGACAT
Accn1-rv	TGGATGAAAGGTGGCTCAGAC
Crym-fw	GTGATTTCAGGAGCGAAGCCT
Crym-rv	AACCAGGTCTTCCACTGCCAT
Wnt10a-fw	CACAGAGACATCCATGCTCGA
Wnt10a-rv	TACGCCGCATGTTCTCCAT
NED-fw	GGACGGCGTGAATACCTACAA
NED-rv	GCTGACATTCGTCCACATCCT

Transfections

HEK293T cells were cultured in 10cm Petri dishes in Dulbecco's Modified Eagle's Medium (Gibco Invitrogen) supplemented with 10% foetal bovine serum (Invitrogen), 100U/ml penicillin and 100µg/ml streptomycin (Invitrogen). One day after seeding, cells were transfected for 3h with a total of 1µg of plasmid DNA, using lipofectamin transfection (Invitrogen).

Luciferase

Cells were harvested 48h after transfection and luciferase activity was measured using the Dual Luciferase® Reporter Assay System (Promega) on a Centro LB 960 luminometer (Berthold Technologies, Vilvoorde, Belgium). For every sample firefly Hes1-luciferase activity was normalized versus TK-Renilla luciferase activity. Statistical significance was determined using Student's t test. A p-value of <0.05 was considered statistically significant. The number of samples per condition was, control, n=9; NICD, n=14; HDAC4, n=14; NICD and HDAC4, n=13.

Results

Microarray analysis of transgenic mice expressing NICD in cortical pyramidal neurons

To investigate Notch1-induced molecular signalling in cerebral cortex, we made use of transgenic mice expressing a constitutively active Notch1-protein (consisting of NICD alone) selectively in cerebral cortex pyramidal neurons, with an expression onset in the early fourth postnatal week [Dahlhaus et al., 2008]. The transgene encoded NICD under the control of the Thy-1 promoter and was preceded by a transcriptional stop cassette flanked by loxP recognition sites. By crossing animals carrying this transgene to G35-3 Cre transgenic mice [Sawtell et al., 2003], offspring was produced in which the stop cassette was excised and transgene expression established in all pyramidal cells in the neocortex and hippocampus.

For microarray analyses, RNA samples were isolated from the cerebral cortex of 9 adult NICD+Cre+ animals and 6 littermate controls (NICD+Cre-, NICD-Cre+ or NICD-Cre-). The RNA samples were pooled per genotype and eight parallel microarray experiments were performed. In half of these experiments a dye swap was performed to avoid dye specific biases.

Statistical analysis of the microarray data revealed a remarkably low number of genes differentially expressed between NICD+Cre+ transgenic mice and littermate controls. By means of ANOVA with Benjamini-Hochberg correction for multiple comparisons, 177 significantly regulated transcripts were identified of which 102 were upregulated in NICD+Cre+ mice and 75 were downregulated (table 1). Only 22 genes were upregulated by more than 25%, 18 genes were downregulated to the same degree (table 2).

Automated categorization of genes with changes in transcript levels did not provide useful information, likely due to the small number of regulated genes. However, upon manual inspection we noticed that especially genes involved in Ras/MAPK signalling were upregulated, including Rasd2, Rasgef1b, Rasgef1c, RIAM, Rph3a, and Mink1, or downregulated such as Grb10 and the Erk target Ets2. Moreover, various genes involved in transcriptional regulation were upregulated (Hes1, XP_359291.1, Atrophin-1 and HDAC4) or downregulated (Ets2 and Nfix). Of these, only Hes1 is a known target of Notch1.

Table 1. Genes expressed significantly different between NICD+Cre+ transgenic animals and controls. A cut-off of p<0.05 (Benjamini-Hochberg corrected ANOVA) was used.

identifier	gene-symbol	description	NICD+Cre+/ control	P-value BH	ENSEMBL
NM_008235	Hes1	hairy and enhancer of split 1	1,66	0,0000	ENSMUSG00000022528
NM_013750	Phlda3	pleckstrin homology-like domain, family A, member 3	1,59	0,0001	ENSMUSG00000041801
NM_011313	S100a6	S100 calcium binding protein A6 (calcyclin)	1,52	0,0001	ENSMUSG00000001025
XM_204287	Rasd2	RASD family, member 2	1,48	0,0001	ENSMUSG00000034472
NM_019456	Apbb1ip	amyloid beta (A4) precursor protein-binding, family B, member 1 interacting protein	1,44	0,0002	ENSMUSG00000026786
NM_029004	Rasgef1c	RasGEF domain family, member 1C	1,35	0,0004	ENSMUSG00000020374
NM_011286	Rph3a	rabphilin 3A	1,34	0,0090	ENSMUSG00000029608
NM_023476	Tinagl	tubulointerstitial nephritis antigen-like	1,31	0,0008	ENSMUSG00000028776
NM_007881	Atn1	atrophin 1	1,31	0,0089	ENSMUSG00000004263
NM_007384	Accn1	amiloride-sensitive cation channel 1, neuronal (degenerin)	1,31	0,0009	ENSMUSG00000020704
NM_001003920	Brsk1	BR serine/threonine kinase 1	1,31	0,0089	ENSMUSG00000035390
XM_359291	XP_359291.1	PREDICTED: similar to ring finger protein 39	1,30	0,0006	ENSMUSG00000036492

identifier	gene-symbol	description	NICD+Cre+/ control	P-value BH	ENSEMBL
	2310067L16Rik	Adult male tongue cDNA, RIKEN full-length enriched library, clone:2310067L16	1,29	0,0008	ENSMUSG00000045567
NM_198250	NP_937893.1	leucine rich repeat containing 4B	1,29	0,0197	ENSMUSG00000047085
NM_207225	Hdac4	histone deacetylase 4	1,29	0,0260	ENSMUSG00000026313
NM_027900	1300003K24Rik	R3H domain protein KIAA1002	1,29	0,0132	ENSMUSG00000025404
NM_016972	Slc7a8	solute carrier family 7 (cationic amino acid transporter, y+ system), member 8	1,28	0,0091	ENSMUSG00000022180
NM_016713;NM_176893	Mink1	misshapen-like kinase 1	1,27	0,0321	ENSMUSG00000020827
NM_145839;NM_181318	Rasgef1b	RasGEF domain family, member 1B	1,27	0,0012	ENSMUSG00000029333
NM_145507;NM_177445	Dars	aspartyl-tRNA synthetase	1,26	0,0090	ENSMUSG00000026356
NM_001008422	AI480556	expressed sequence AI480556	1,26	0,0071	ENSMUSG00000038406
NM_007591	Calr	calreticulin	1,26	0,0231	ENSMUSG00000003814
			1,25	0,0442	ENSMUSG00000021095
NM_177282	Mical2	microtubule associated monoxygenase, calponin and LIM domain containing 2	1,25	0,0037	ENSMUSG00000038244
XM_619970	Col24a1	procollagen, type XXIV, alpha 1	1,24	0,0041	ENSMUSG00000028197
NM_178396	Car12	carbonic anyhydrase 12	1,239	0,0025	ENSMUSG00000032373
NM_198411	2610204M08Rik	RIKEN cDNA 2610204M08 gene (2610204M08Rik), mRNA	1,239	0,0084	ENSMUSG00000037679

identifier	gene-symbol	description	NICD+Cre+/ control	P-value BH	ENSEMBL
NM_198618	Dlgap3	discs, large (Drosophila) homolog-associated protein 3	1,238	0,0285	ENSMUSG00000042388
NM_021287	Spnb3	spectrin beta 3	1,236	0,0082	ENSMUSG00000067889
NM_009854	Cd7	CD7 antigen	1,233	0,0090	ENSMUSG00000025163
NM_008451	Klc2	kinesin light chain 2	1,231	0,0190	ENSMUSG00000024862
NM_026345	Mansc1	MANSC domain containing 1	1,23	0,0199	ENSMUSG00000032718
NM_033218	Srebf2	sterol regulatory element binding factor 2	1,229	0,0202	ENSMUSG00000022463
NM_172911	D8Ertd82e	MFLJ00269 protein (Fragment)	1,227	0,0053	ENSMUSG00000050271
NM_009655	Alcam	activated leukocyte cell adhesion molecule	1,226	0,0055	ENSMUSG00000022636
NM_013879	Cabp1	calcium binding protein 1	1,22	0,0162	ENSMUSG00000029544
XM_489730	Rtdr1	rhabdoid tumor deletion region gene 1	1,219	0,0114	ENSMUSG00000009070
	Maz	MYC-associated zinc finger protein (purine-binding transcription factor)	1,217	0,0240	ENSMUSG00000030678
NM_007416	Adra1b	adrenergic receptor, alpha 1b	1,215	0,0132	ENSMUSG00000050541
NM_009923	Cnp1	cyclic nucleotide phosphodiesterase 1	1,214	0,0042	ENSMUSG00000006782
NM_009497	Vamp2	vesicle-associated membrane protein 2	1,213	0,0260	ENSMUSG00000020894
NM_008372	Il7r	interleukin 7 receptor	1,212	0,0321	ENSMUSG00000003882
NM_013509	Eno2	enolase 2, gamma neuronal	1,212	0,0311	ENSMUSG00000004267

identifier	gene-symbol	description	NICD+Cre+/ control	P-value BH	ENSEMBL
NM_028250	Acbd6	acyl-Coenzyme A binding domain containing 6	1,212	0,0071	ENSMUSG00000033701
NM_177994	C030046I01Rik	RIKEN cDNA C030046I01 gene (C030046I01Rik), mRNA	1,212	0,0255	ENSMUSG00000035781
NM_172498	Ptk2b	PTK2 protein tyrosine kinase 2 beta	1,211	0,0173	ENSMUSG00000059456
NM_008048	Igfbp7	insulin-like growth factor binding protein 7	1,209	0,0037	ENSMUSG00000036256
NM_009305	Syp	synaptophysin	1,208	0,0162	ENSMUSG00000031144
NM_182993	Slc17a7	solute carrier family 17 (sodium-dependent inorganic phosphate cotransporter), member 7	1,208	0,0486	ENSMUSG00000045228
XM_484289	Ell2	elongation factor RNA polymerase II 2	1,206	0,0089	ENSMUSG00000001542
NM_018763	Chst2	carbohydrate sulfotransferase 2	1,204	0,0173	ENSMUSG00000033350
NM_130863	Adrbk1	adrenergic receptor kinase, beta 1	1,203	0,0386	ENSMUSG00000024858
NM_177639	Dlgap1	discs, large (Drosophila) homolog-associated protein 1	1,203	0,0375	ENSMUSG00000003279
NM_021287	Spnb3	spectrin beta 3	1,202	0,0255	ENSMUSG00000067889
NM_001099632.1	XP_359291.1	PREDICTED: similar to ring finger protein 39	1,202	0,0074	ENSMUSG00000036492
NM_001005511		lemur tyrosine kinase 3 (Lmtk3), mRNA	1,202	0,0480	ENSMUSG00000062044
NM_026823	Arl10b	ADP-ribosylation factor-like 10B	1,201	0,0322	ENSMUSG00000026426
NM_016782	Cntnap1	contactin associated protein 1	1,198	0,0268	ENSMUSG00000017167

identifier	gene-symbol	description	NICD+Cre+/ control	P-value BH	ENSEMBL
NM_027519	6330406I15Rik	RIKEN cDNA 6330406I15 gene (6330406I15Rik), mRNA	1,197	0,0162	ENSMUSG00000029659
NM_183315	Ctxn1	cortexin 1	1,197	0,0181	ENSMUSG00000048644
NM_010758	Mag	myelin-associated glycoprotein	1,196	0,0149	ENSMUSG00000036634
NM_178090;NM_153405	Drbp1	developmentally regulated RNA binding protein 1	1,195	0,0371	ENSMUSG00000042369
NM_021286	Sez6	seizure related gene 6	1,194	0,0181	ENSMUSG00000000632
NM_019869	Rbm14	RNA binding motif protein 14	1,194	0,0162	ENSMUSG00000006456
NM_153166	Cpne5	copine V	1,194	0,0275	ENSMUSG00000024008
NM_053272	Dhcr24	24-dehydrocholesterol reductase	1,192	0,0311	ENSMUSG00000034926
NM_029935	4631426J05Rik	N-acetylgalactosamine 4-sulfate 6-O-sulfotransferase	1,192	0,0197	ENSMUSG00000030930
NM_175012	Grp	gastrin releasing peptide	1,192	0,0154	ENSMUSG00000024517
XM_620246	XP_620246.1	PREDICTED: myosin XVIIIb	1,192	0,0346	ENSMUSG00000044918
NM_133825	D1Ertd622e		1,191	0,0164	ENSMUSG00000044768
NM_008226	Hcn2	hyperpolarization-activated, cyclic nucleotide-gated K+ 2	1,191	0,0365	ENSMUSG00000020331
NM_207583	6430517E21Rik	BMP/retinoic acid-inducible neural-specific protein 2	1,189	0,0162	ENSMUSG00000004031
NM_138686;NM_001004455	Cys1	ribonucleotide reductase M2	1,189	0,0188	ENSMUSG00000062563
NM_029186	4930538D17Rik	RIKEN cDNA 4930538D17 gene (4930538D17Rik), mRNA	1,188	0,0167	ENSMUSG00000025227
NM_010592	Jund1	Jun proto-oncogene related gene d1	1,187	0,0496	ENSMUSG00000049389

identifier	gene-symbol	description	NICD+Cre+/ control	P-value BH	ENSEMBL
NM_020006	Cdc42ep4	CDC42 effector protein (Rho GTPase binding) 4	1,187	0,0129	ENSMUSG00000041598
NM_173403	NP_775579.1		1,187	0,0485	ENSMUSG00000029219
NM_007458	Ap2a1	adaptor protein complex AP-2, alpha 1 subunit	1,185	0,0208	ENSMUSG00000060279
NM_008528	Blnk	B-cell linker	1,185	0,0318	ENSMUSG00000061132
NM_019875;NM_177876	Abcb9	ATP-binding cassette, sub-family B (MDR/TAP), member 9	1,185	0,0162	ENSMUSG00000029408
	1200016G03Rik	NOD-derived CD11c +ve dendritic cells cDNA, RIKEN full-length enriched library	1,18	0,0240	ENSMUSG00000037185
NM_009451	Tubb4	tubulin, beta 4	1,179	0,0453	ENSMUSG00000062591
NM_011072	Pfn1	profilin 1	1,177	0,0253	ENSMUSG00000018293
NM_007463	Apeg1	aortic preferentially expressed gene 1	1,177	0,0431	ENSMUSG00000026207
NM_031406	Slc12a9	solute carrier family 12 (potassium/chloride transporters), member 9	1,176	0,0260	ENSMUSG00000037344
NM_008940	Prss19	protease, serine, 19 (neuropsin)	1,175	0,0255	ENSMUSG00000064023
NM_008770	Cldn11	claudin 11	1,174	0,0295	ENSMUSG00000037625
	OST2_MOUSE	Heparan sulfate glucosamine 3-O-sulfotransferase 2 (EC 2.8.2.29)	1,174	0,0306	ENSMUSG00000046321
NM_198192	Gpr103	G protein-coupled receptor 103	1,172	0,0453	ENSMUSG00000058400
NM_054095	Efcbp2	EF hand calcium binding protein 2	1,17	0,0152	ENSMUSG00000031837
	Kalrn	kalirin, RhoGEF kinase	1,17	0,0447	ENSMUSG00000057487

identifier	gene-symbol	description	NICD+Cre+/ control	P-value BH	ENSEMBL
NM_008614	Mobp	myelin-associated oligodendrocytic basic protein	1,169	0,0260	ENSMUSG00000032517
XM_181420	Cgref1	cell growth regulator with EF hand domain 1	1,169	0,0321	ENSMUSG00000029161
NM_013746	Plekhb1	pleckstrin homology domain containing, family B (evectins) member 1	1,168	0,0275	ENSMUSG00000030701
NM_001024955	Pik3r1	phosphatidylinositol 3-kinase, regulatory subunit, polypeptide 1 (p85 alpha)	1,164	0,0340	ENSMUSG00000041417
NM_144828	Ppp1r1b	protein phosphatase 1, regulatory (inhibitor) subunit 1B	1,164	0,0364	ENSMUSG00000061718
NM_029815	Bcas1	breast carcinoma amplified sequence 1	1,163	0,0402	ENSMUSG00000013523
NM_001008231	Daam2	dishevelled associated activator of morphogenesis 2	1,163	0,0494	ENSMUSG00000040260
NM_008800	Pde1b	phosphodiesterase 1B, Ca2+-calmodulin dependent	1,162	0,0453	ENSMUSG00000022489
NM_153534	Adcy2	adenylate cyclase 2	1,162	0,0380	ENSMUSG00000021536
NM_173437	Nav1	neuron navigator 1	1,158	0,0480	ENSMUSG00000009418
NM_198424	BC061259	cDNA sequence BC061259	1,154	0,0310	ENSMUSG00000043964
NM_013587	Lrpap1	low density lipoprotein receptor-related protein associated protein 1	0,864	0,0480	ENSMUSG00000029103

identifier	gene-symbol	description	NICD+Cre+/ control	P-value BH	ENSEMBL
NM_028099	Dusp11	dual specificity phosphatase 11 (RNA/RNP complex 1-interacting)	0,861	0,0494	ENSMUSG00000030002
NM_011585	Tia1	cytotoxic granule-associated RNA binding protein 1	0,859	0,0398	ENSMUSG00000029997
NM_025926;NM_027287	Dnajb4	DnaJ (Hsp40) homolog, subfamily B, member 4	0,857	0,0455	ENSMUSG00000028035
NM_010380	H2-L	histocompatibility 2, D region locus 1	0,856	0,0350	ENSMUSG00000036861
NM_010444	Nr4a1	nuclear receptor subfamily 4, group A, member 1	0,855	0,0295	ENSMUSG00000023034
	Q3U781_ MOUSE	Bone marrow macrophage cDNA, RIKEN full-length enriched library, product:splicing factor	0,854	0,0431	ENSMUSG00000034437
NM_172618	Btbd9	BTB (POZ) domain containing 9	0,854	0,0311	ENSMUSG00000062202
NM_013663	Sfrs3	splicing factor, arginine/serine-rich 3 (SRp20)	0,854	0,0375	ENSMUSG00000045786
NM_146083	Sfrs7	splicing factor, arginine/serine-rich 7	0,853	0,0275	ENSMUSG00000024097
NM_175031	Stk36	serine/threonine kinase 36 (fused homolog, Drosophila)	0,852	0,0255	ENSMUSG00000033276
			0,851	0,0442	ENSMUSG00000051566
NM_011212	Ptpre	protein tyrosine phosphatase, receptor type, E	0,85	0,0322	ENSMUSG00000041836
NM_144817	Camk1g	calcium/calmodulin-dependent protein kinase I gamma	0,848	0,0260	ENSMUSG00000016179

identifier	gene-symbol	description	NICD+Cre+/ control	P-value BH	ENSEMBL
NM_029653	Dapk1	death associated protein kinase 1	0,848	0,0238	ENSMUSG00000021559
NM_009700	Aqp4	aquaporin 4	0,848	0,0285	ENSMUSG00000024411
NM_009786	Cacybp	calcyclin binding protein	0,847	0,0371	ENSMUSG00000014226
	Rtf1	Rtf1, Paf1/RNA polymerase II complex component, homolog (S. cerevisiae)	0,844	0,0181	ENSMUSG00000027304
	Q6LCX0_ MOUSE	Mus musculus clone NCD40 LINE-1 element ORF1 (Fragment)	0,844	0,0296	ENSMUSG00000057331
NM_153457;NM_001007596	Rtn1	reticulon 1	0,843	0,0321	ENSMUSG00000021087
XM_283936	5730406M06Rik	8 days embryo whole body cDNA, RIKEN full-length enriched library, product:SR rich protein homolog	0,842	0,0162	ENSMUSG00000028248
NM_025693	Tmem41a	transmembrane protein 41a	0,842	0,0350	ENSMUSG00000022856
NM_021305	Sec61a2	Sec61, alpha subunit 2 (S. cerevisiae)	0,842	0,0340	ENSMUSG00000025816
NM_029248	4930553M18Rik	RIKEN cDNA 4930553M18 gene (4930553M18Rik), transcript variant 2, mRNA	0,842	0,0189	ENSMUSG00000031939
	Q3USP3_ MOUSE	Adult male corpora quadrigemina cDNA, RIKEN full-length enriched library, product:hypothetical protein	0,842	0,0173	ENSMUSG00000044224
NM_028765	Acoxl	acyl-Coenzyme A oxidase-like	0,841	0,0202	ENSMUSG00000027380

identifier	gene-symbol	description	NICD+Cre+/ control	P-value BH	ENSEMBL
NM_178888	Garnl3	GTPase activating RANGAP domain-like 3	0,841	0,0198	ENSMUSG00000038860
	A230054D04Rik	RIKEN cDNA A230054D04 gene	0,841	0,0209	ENSMUSG00000050223
NM_008963	NP_032989.1	prostaglandin H2 D-isomerase	0,839	0,0172	ENSMUSG00000015090
NM_053078	D0H4S114	DNA segment, human D4S114	0,839	0,0179	ENSMUSG00000042834
NM_175692	A930034L06Rik	RIKEN cDNA A930034L06 gene (A930034L06Rik), mRNA	0,839	0,0240	ENSMUSG00000044349
NM_009905	Clk1	CDC-like kinase 1	0,838	0,0198	ENSMUSG00000026034
NM_175480	Zfp612	zinc finger protein 612	0,838	0,0162	ENSMUSG00000044676
NM_023665	D4Wsu53e	18-day embryo whole body cDNA, RIKEN full-length enriched library, product:similar to HT033	0,835	0,0093	ENSMUSG00000037266
XM_622627	XM_622627.1	similar to cytoplasmic beta-actin (LOC547246), mRNA	0,834	0,0398	ENSMUSG00000060781
NM_024193	Nol5a	nucleolar protein 5A	0,834	0,0183	ENSMUSG00000027405
NM_022310	Hspa5	heat shock 70kD protein 5 (glucose-regulated protein)	0,83	0,0132	ENSMUSG00000026864
NM_022316	Smoc1	SPARC related modular calcium binding 1	0,829	0,0134	ENSMUSG00000021136
NM_011211;NM_001014288	Ptprd	protein tyrosine phosphatase, receptor type, D	0,826	0,0170	ENSMUSG00000028399
NM_023131	Rce1	RCE1 homolog, prenyl protein peptidase (S. cerevisiae)	0,825	0,0321	ENSMUSG00000024889
XM_127032	Fbxo33	F-box only protein 33	0,824	0,0087	ENSMUSG00000035329

identifier	gene-symbol	description	NICD+Cre+/ control	P-value BH	ENSEMBL
NM_016809	Rbm3	RNA binding motif protein 3	0,824	0,0061	ENSMUSG00000031167
NM_010514	Igf2	insulin-like growth factor 2	0,823	0,0162	ENSMUSG00000048583
			0,822	0,0089	ENSMUS-ESTG00000020631
NM_175631	Cbln4	cerebellin 4 precursor protein	0,818	0,0041	ENSMUSG00000067578
			0,818	0,0492	ENSMUSG00000046782
NM_010345	Grb10	growth factor receptor bound protein 10	0,815	0,0037	ENSMUSG00000020176
NM_170778	Dpyd	dihydropyrimidine dehydrogenase	0,814	0,0055	ENSMUSG00000033308
NM_008963	NP_032989.1	prostaglandin H2 D-isomerase	0,813	0,0041	ENSMUSG00000015090
NM_008963	NP_032989.1	prostaglandin H2 D-isomerase	0,812	0,0028	ENSMUSG00000015090
NM_018883	Camkk1	calcium/calmodulin-dependent protein kinase kinase 1, alpha	0,81	0,0052	ENSMUSG00000020785
NM_010305	Gnai1	guanine nucleotide binding protein, alpha inhibiting 1	0,807	0,0061	ENSMUSG00000057614
NM_144551	Trib2	tribbles homolog 2 (Drosophila)	0,805	0,0024	ENSMUSG00000020601
NM_013694	Tnp2	transition protein 2	0,803	0,0052	ENSMUSG00000043050
NM_008664	Myom2	myomesin 2	0,802	0,0064	ENSMUSG00000031461
NM_177185	D130059P03Rik	RIKEN cDNA D130059P03 gene (D130059P03Rik), mRNA (ubinuclein2)	0,801	0,0300	ENSMUSG00000038538
			0,80	0,0025	ENSMUSG00000067730
NM_010930	Nov	nephroblastoma overexpressed gene	0,80	0,0041	ENSMUSG00000037362

identifier	gene-symbol	description	NICD+Cre+/ control	P-value BH	ENSEMBL
NM_016669	Crym	crystallin, mu	0,79	0,0012	ENSMUSG00000030905
NM_011809	Ets2	E26 avian leukemia oncogene 2, 3' domain	0,79	0,0025	ENSMUSG00000022895
NM_024200	Mfn1	mitofusin 1	0,78	0,0016	ENSMUSG00000027668
NM_013626	Pam	peptidylglycine alpha-amidating monooxygenase	0,78	0,0407	ENSMUSG00000026335
NM_175514	D430039N05Rik	RIKEN cDNA D430039N05 gene (D430039N05Rik), mRNA	0,78	0,0257	ENSMUSG00000048388
NM_170684	NP_733785.1	copine 7 protein	0,77	0,0012	ENSMUSG00000034796
NM_144797	Metrnl	meteorin, glial cell differentiation regulator-like	0,77	0,0009	ENSMUSG00000039208
NM_010345	Grb10	growth factor receptor bound protein 10	0,77	0,0257	ENSMUSG00000020176
NM_010906	Nfix	nuclear factor I/X	0,77	0,0327	ENSMUSG00000001911
NM_028118	Wdsub1	WD repeat, SAM and U-box domain containing 1	0,76	0,0009	ENSMUSG00000026988
NM_009518	Wnt10a	wingless related MMTV integration site 10a	0,75	0,0005	ENSMUSG00000026167
NM_183321	BC053749	cDNA sequence BC053749	0,71	0,0209	ENSMUSG00000036864
NM_146440	Olfr919	olfactory receptor 919	0,71	0,0162	ENSMUSG00000056961
NM_011022	Ott	ovary testis transcribed	0,71	0,0170	ENSMUSG00000056861
NM_029879	D13Bwg1146e	R7 binding protein	0,69	0,0027	ENSMUSG00000021719
XM_899867	Cdkn3	cyclin-dependent kinase inhibitor 3	0,64	0,0001	ENSMUSG00000037628

Table 2. Genes expressed significantly different between NICD+Cre+ transgenic animals and controls. A cut-off of p<0.05 (Benjamini-Hochberg corrected ANOVA) and 1.25 fold change was used.

Identifier	Symbol	Description	NICD+Cre+/ control	P-value BH	ENSEMBL-identifier
NM_008235	Hes1	hairy and enhancer of split 1	1.66	0.0000	ENSMUSG00000022528
NM_013750	Phlda3	pleckstrin homology-like domain, family A, member 3	1.59	0.0001	ENSMUSG00000041801
NM_011313	S100a6	S100 calcium binding protein A6 (calcyclin)	1.52	0.0001	ENSMUSG00000001025
XM_204287	Rasd2	RASD family, member 2	1.48	0.0001	ENSMUSG00000034472
NM_019456	Apbb1ip	amyloid beta (A4) precursor protein-binding, family B, member 1 interacting protein (RIAM)	1.44	0.0002	ENSMUSG00000026786
NM_029004	Rasgef1c	RasGEF domain family, member 1C	1.35	0.0004	ENSMUSG00000020374
NM_011286	Rph3a	rabphilin 3A	1.34	0.0090	ENSMUSG00000029608
NM_023476	Tinagl	tubulointerstitial nephritis antigen-like	1.31	0.0008	ENSMUSG00000028776
NM_007881	Atn1	atrophin 1	1.31	0.0089	ENSMUSG00000004263
NM_007384	Accn1	amiloride-sensitive cation channel 1, neuronal (degenerin)	1.31	0.0009	ENSMUSG00000020704
NM_001003920	Brsk1	BR serine/threonine kinase 1	1.31	0.0089	ENSMUSG00000035390
XM_359291	XP_359291.1	PREDICTED: similar to ring finger protein 39	1.30	0.0006	ENSMUSG00000036492
	2310067L16Rik	Adult male tongue cDNA, RIKEN full-length enriched library, clone:2310067L16	1.29	0.0008	ENSMUSG00000045567

Identifier	Symbol	Description	NICD+Cre+/ control	P-value BH	ENSEMBL-identifier
NM_198250	NP_937893.1	leucine rich repeat containing 4B	1.29	0.0197	ENSMUSG00000047085
NM_207225	Hdac4	histone deacetylase 4	1.29	0.0260	ENSMUSG00000026313
NM_027900	1300003K24Rik	R3H domain protein KIAA1002	1.29	0.0132	ENSMUSG00000025404
NM_016972	Slc7a8	solute carrier family 7 (cationic amino acid transporter, y+ system), member 8	1.28	0.0091	ENSMUSG00000022180
NM_016713;NM_176893	Mink1	misshapen-like kinase 1	1.27	0.0321	ENSMUSG00000020827
NM_145839;NM_181318	Rasgef1b	RasGEF domain family, member 1B	1.27	0.0012	ENSMUSG00000029333
NM_145507;NM_177445	Dars	aspartyl-tRNA synthetase	1.26	0.0090	ENSMUSG00000026356
NM_001008422	AI480556	expressed sequence AI480556	1.26	0.0071	ENSMUSG00000038406
NM_007591	Calr	calreticulin	1.26	0.0231	ENSMUSG00000003814
			0.80	0.0025	ENSMUSG00000067730
NM_010930	Nov	nephroblastoma overexpressed gene	0.80	0.0041	ENSMUSG00000037362
NM_016669	Crym	crystallin, mu	0.79	0.0012	ENSMUSG00000030905
NM_011809	Ets2	E26 avian leukemia oncogene 2, 3' domain	0.79	0.0025	ENSMUSG00000022895
NM_024200	Mfn1	mitofusin 1	0.78	0.0016	ENSMUSG00000027668
NM_013626	Pam	peptidylglycine alpha-amidating monooxygenase	0.78	0.0407	ENSMUSG00000026335
NM_175514	D430039N05Rik	RIKEN cDNA D430039N05 gene (D430039N05Rik), mRNA	0.78	0.0257	ENSMUSG00000048388
NM_170684	NP_733785.1	copine 7 protein	0.77	0.0012	ENSMUSG00000034796

Identifier	Symbol	Description	NICD+Cre+/ control	P-value BH	ENSEMBL-identifier
NM_144797	Metrnl	meteorin, glial cell differentiation regulator-like	0.77	0.0009	ENSMUSG00000039208
NM_010345	Grb10	growth factor receptor bound protein 10	0.77	0.0257	ENSMUSG00000020176
NM_010906	Nfix	nuclear factor I/X	0.77	0.0327	ENSMUSG00000001911
NM_028118	Wdsub1	WD repeat, SAM and U-box do-main containing 1	0.76	0.0009	ENSMUSG00000026988
NM_009518	Wnt10a	wingless related MMTV integration site 10a	0.75	0.0005	ENSMUSG00000026167
NM_183321	BC053749	cDNA sequence BC053749	0.71	0.0209	ENSMUSG00000036864
NM_146440	Olfr919	olfactory receptor 919	0.71	0.0162	ENSMUSG00000056961
NM_011022	Ott	ovary testis transcribed	0.71	0.0170	ENSMUSG00000056861
NM_029879	D13Bwg1146e	R7 binding protein	0.69	0.0027	ENSMUSG00000021719
XM_899867	Cdkn3	cyclin-dependent kinase inhibitor 3	0.64	0.0001	ENSMUSG00000037628

Other genes regulated in NICD transgenic animals that could not be grouped but potentially play a role in cortical plasticity or degeneration included Phlda3 (a p53 regulated repressor of Akt) Cdkn3 (an inhibitor of the kinase Cdk2), S100a6 (a calcium binding protein) and Brsk1 (a kinase involved in axon outgrowth and vesicle release).

Confirmation of microarray results by quantitative RT-PCR

To confirm the microarray results, RNA was isolated from additional animals and quantitative RT-PCR was performed for a number of genes regulated significantly, and displaying a difference of at least 25% between control animals and transgenics. Genes selected included representatives of the groups mentioned above and others likely interesting for understanding plasticity. Compared to control littermates (set to 1) NICD+Cre+ animals showed increased expression of Hes1 (2.47 ± 0.26 in transgenics vs 1 ± 0.08 in littermate controls; $p<0.001$; figure 1 and figure 2c), RIAM (2.20 ± 0.22 vs 1 ± 0.07; $p<0.001$; figure 1 and figure 2e), S100a6 (1.61 ± 0.11 vs 1 ± 0.08; $p<0.001$; figure 1 and figure 2g), Rasgef1c (1.78 ± 0.12 vs 1 ± 0.11; $p<0.001$; figure 1), Phlda3 (2.11 ± 0.35 vs 1 ± 0.10; $p<0.01$; figure 1) and HDAC4 (1.47 ± 0.09 vs 1 ± 0.11; $p=0.001$; figure 1).

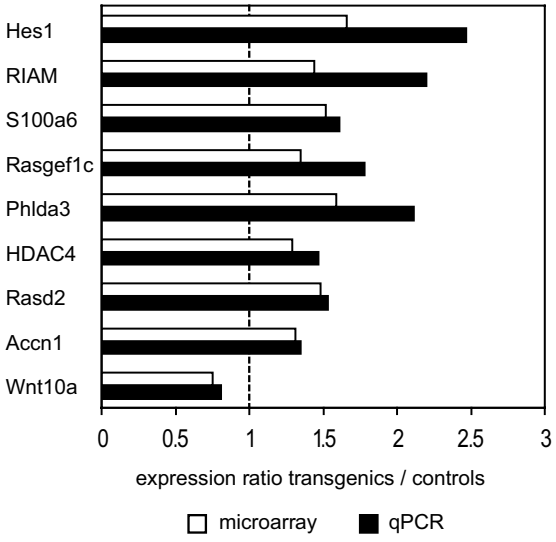

Figure 1. Confirmation of expression of selected genes by quantitative RT-PCR. Representation of fold changes of selected genes in NICD+Cre+ animals compared to controls, for both microarray (white) and qPCR (black).

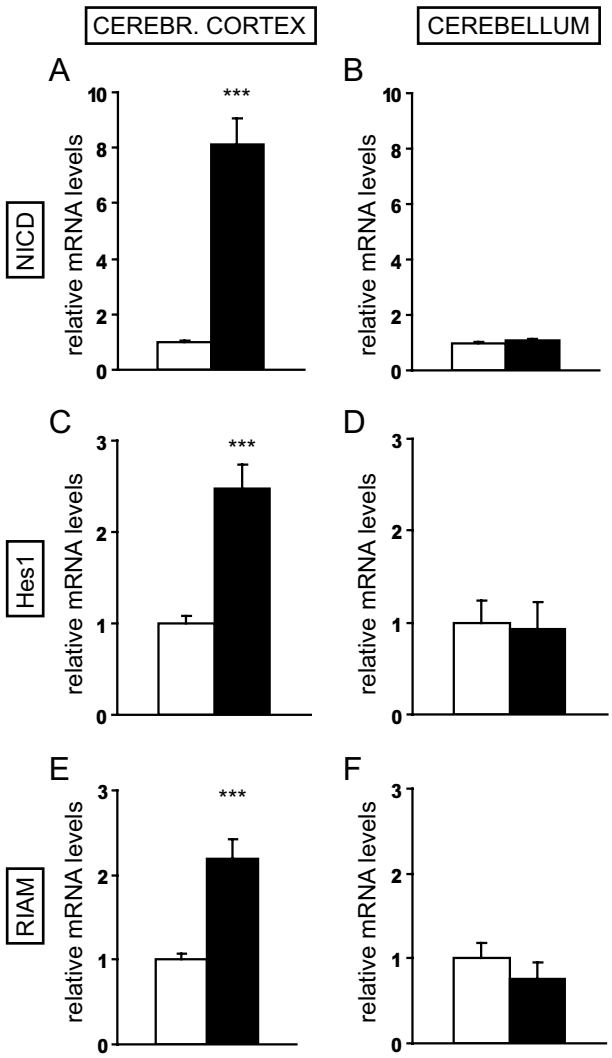

Figure 2 (continued on next page). Differential gene expression between NICD+Cre+ transgenics and controls is restricted to the cerebral cortex. Cre expression occurs in the cerebral cortex but not in the cerebellum. To show that modulation of transcription in transgenic animals occurs only in the brain region where Cre is expressed, quantitative RT-PCR was performed in both the cerebral cortex and cerebellum. A-B) Expression of the Notch intracellular domain is increased in the cerebral cortex of NICD+Cre+ transgenic animals, but not in the cerebellum. The same is true for Hes1 (C-D), RIAM (E-F) and S100a6 (G-H). I) Expression of the Notch extracellular domain (NED) is unchanged in the cerebral cortex of NICD+Cre+ transgenic animals, demonstrating that increased NICD expression in the cerebral cortex of NICD+Cre+ transgenic animals (A) reflects transgene expression. Error bars indicate SEM. *** $p<0.001$. Data on cortex: 19 controls, 22 transgenics. Data on cerebellum: 8 controls, 8 transgenics.

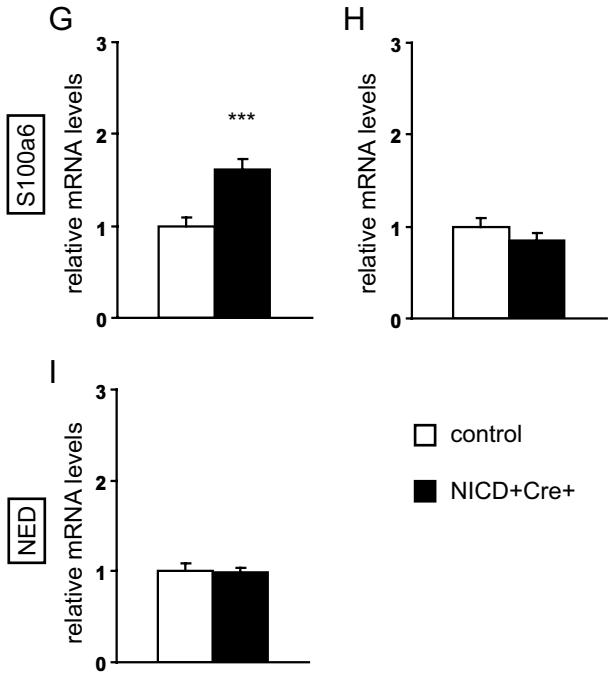

Figure 2 continued.

RT-PCR on three other transcripts showed a trend towards regulation in the same direction as the microarray experiments, although these differences were not significant. This was true for Rasd2 (1.53 ± 0.33 in transgenics compared to 1 ± 0.13 in littermate controls; p=0.09; figure 1), Accn1 (1.35 ± 0.23 vs 1 ± 0.19; p=0.13; figure 1) and Wnt10a (0.81 ± 0.11 vs 1 ± 0.16; p=0.15; figure 1). Also NICD expression was increased (8.12 ± 0.91 vs 1 ± 0.05; p<0.001; figure 2a). To show that this specifically represented NICD transgene expression, we also quantified NICD expression in the retina [Dahlhaus et al., 2008] and cerebellum, where transgene expression does not occur. Indeed, in the cerebellum NICD expression was not increased in transgenics compared to controls (1.09 ± 0.05 vs 1 ± 0.05; p=0.41; figure 2b). Additionally, we quantified expression of the Notch extracellular domain (NED) and found that as anticipated, expression of the extracellular part of Notch was unaffected (0.98 ± 0.06 vs 1 ± 0.09; p=0.88; figure 2i).

Regulation of transcripts by Notch was restricted to the brain regions where transgene expression occurred. Expression of Hes1, RIAM and S100a6 was not changed in the cerebellum of NICD+Cre+ animals (figure 2d, 2f and 2h). This showed that the observed effects were specifically due to constitutive activity of the Notch pathway brought about by transgene expression.

HDAC4 inhibits Notch-mediated expression of Hes1

The number of genes of which expression levels were changed by overexpression of NICD appeared relatively small. Interestingly, among the upregulated genes we noticed a class IIa HDAC, HDAC4. Class IIa HDACs are known to interact with HDAC1 (a class I HDAC) and CtBP, both inhibitors of Notch1-signalling. We therefore hypothesized that HDAC4 may form part of a feedback loop restricting Notch-signalling.

To analyse this possibility, we investigated whether overexpression of HDAC4 inhibits Notch1-mediated Hes1 expression. HEK293T cells were transfected with a construct containing the Hes1-promoter driving firefly-derived luciferase expression. A construct encoding the TK promoter driving Renilla-derived luciferase was used as a normalisation control, not affected by Notch pathway signalling. The influence of NICD and HDAC4 was tested by cotransfecting constructs encoding these proteins, while a GFP construct served both to determine transfection efficiency and to balance the total amount of transfected DNA.

As expected, expression of NICD increased promoter activity of its primary downstream target, Hes1 (2.65 ± 0.33 relative to control levels set to 1 ± 0.15; $p=0.001$; figure 3). HDAC4 expression alone resulted in reduced Hes1 promoter activity (0.48 ± 0.07; $p=0.002$ compared to control; figure 3). Co-expression of HDAC4 with NICD (1.06 ± 0.19; figure 3) prevented the increased Hes1 activity induced by NICD ($p=0.0004$), rendering it similar to control levels ($p=0.83$; figure 3). Together, these data indeed confirm that HDAC4 inhibits Notch1-mediated transcription of Hes1.

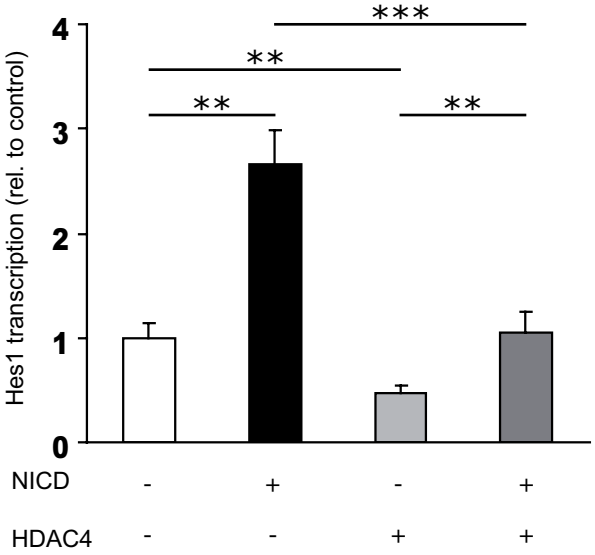

Figure 3. HDAC4 inhibits Notch-mediated transcription. Expression of NICD in HEK293 cells resulted in increased expression of its primary downstream target, Hes1, determined by using a co-expressed Hes1-luciferase reporter. HDAC4 reduced Hes1 expression under control conditions, and also prevented the increased Hes1 expression induced by Notch. Error bars indicate SEM. ** $p<0.01$; *** $p<0.001$.

Discussion

In this study we aimed to identify and characterize transcripts regulated by Notch1-signalling in cerebral cortical pyramidal neurons and identify potential mediators of its effects on structural and functional plasticity. To this end, we used transgenic animals expressing NICD in pyramidal neurons of the neocortex, starting 3-4 weeks after birth. In this same mouse model, we have shown previously that cortical plasticity is affected by Notch1-signalling, both in vitro and in vivo [Dahlhaus et al., 2008]. Making use of microarray analysis and quantitative RT-PCR, we compared gene expression levels in these mice with control animals. A surprisingly small number of transcripts was found to be regulated by more than 25% as a result of enhanced Notch1-signalling. We noticed that although not all these genes could be grouped in functional categories, there was an overrepresentation of two groups of genes: those involved in the Ras/MAPK pathway and those mediating transcriptional regulation. Of the genes that could not be classified in these groups, some are worthy of note due to their potential involvement in regulating cortical plasticity or neurodegeneration or possible cross-talk with Notch1-signalling. Of particular interest are Phlda3, Cdkn3, s100a6 and Brsk1. Phlda3 is a recently discovered p53 regulated repressor of Akt-signalling [Kawase et al., 2009], a signalling pathway intertwined with Notch-signalling and well known to regulate synaptic plasticity and neuronal morphology. Cdkn3 is an inhibitor of Cdk2, a kinase activated by Notch1 [Ronchini et al., 2001]. S100a6 is a calcium binding protein potentially involved in the pathogenesis of Alzheimer's disease and found to be upregulated in APP transgenic animals [Boom et al., 2004]. Last, Brsk1 is a kinase recently discovered to be involved in neuronal polarity, axon outgrowth [Kishi et al., 2005; Barnes et al., 2007] and vesicle release [Inoue et al., 2006].

The Ras/Mapk- and Notch1-signalling pathways are known to interact at various levels, and can result in antagonism [Yoo et al., 2004; Hasson et al., 2005; Kawamura et al., 2005] or cooperation [Katz et al., 1995] depending on the system and cell type. We found that in our NICD transgenic animals, more genes stimulating Ras signalling were upregulated (5 genes: Rasgef1b, Rasgef1c, Riam, Rph3a, and Mink1) than downregulated (2 genes: Grb10 and Ets2) indicating that in post-synaptic neurons Ras- and Notch1-signalling may be predominantly cooperative. An especially interesting gene among these is Riam, also known as amyloid beta precursor protein-binding, family B, member 1 (Apbb1ip). As the name suggests, RIAM interacts with the APP binding protein Fe65 [Ermekova et al., 1997] and may be

involved in APP-signalling which has extensive cross-talk with the Notch1 pathway [Fischer et al., 2005]. Moreover, RIAM is involved in integrin-mediated adhesion [Lafuente et al., 2004; Lee et al., 2009] and actin-cytoskeleton dynamics [Lafuente et al., 2004; Jenzora et al., 2005] and thus at an excellent position to regulate synaptic plasticity and neurite outgrowth.

The genes encoding transcriptional regulators that were upregulated in NICD transgenic mice include the canonical Notch1 target Hes1, Atrophin-1, HDAC4 and the obscure gene XP_545466, ("similar to ring finger protein 39") of which no functional data exists. Hes1, Atrophin-1 and HDAC4 all have direct or indirect relations to Notch1, neurite outgrowth, synaptic plasticity or neurodegeneration. Hes1 is the best-known target of Notch1-signalling and has previously been found to regulate neurite outgrowth. It may thus be an effector in the plasticity phenotype of NICD transgenic animals [Dahlhaus et al., 2008]. Atrophin-1 is a transcriptional corepressor, which may interact with Notch1-signalling through two different signalling cascades. Outside of the nucleus, Atrophin-1 interacts with the ubiquitin E3 ligase AIP4 which is a regulator of Notch1 degradation. Moreover, the gene encoding Atrophin-1 itself is implicated in the neurodegenerative disease Dentatorubral-Pallidoluysian atrophy, probably through transcriptional repression involving class I HDAC's. Interestingly, class I HDAC's also inhibit Notch-induced molecular signalling [Kao et al., 1998]. Whether Atrophin-1 indeed downregulates Notch1 through these two mechanisms is not known. We do find however that another HDAC, HDAC4, is also upregulated in NICD transgenic animals and that it has the capacity to inhibit Notch1 mediated gene transcription, thus providing a negative feedback signal.

We believe that this finding may explain why only a limited number of genes was found to be regulated by NICD overexpression, and clarify our previous observation that increasing levels of Notch1 expression during the development of our NICD transgenic does not further increase expression levels of Hes1 [Dahlhaus et al., 2008]. HDAC4 is a type II member of the HDAC family, members of which are believed to regulate transcription by recruiting other nuclear suppressors to specific genes. HDAC4 contains a binding site for CtBP [Zhang et al., 2001], which acts as a co-repressor for Notch target genes and links HDAC to the transcriptional repressor Hairless in Drosophila [Lai, 2002] and SHARP in mammals [Oswald et al., 2005]. Thus, NICD expression in pyramidal neurons of the neocortex upregulates HDAC4 and possibly other transcriptional repressors that play a potential role in mediating

negative feedback and may represent a mechanism by which Notch1 mediated gene expression is maintained at physiological levels.

Apart from restricting Notch1 activity, this regulation of HDAC4 expression may also affect plasticity in the visual cortex of NICD transgenic animals. It has recently been shown that histone acetylation decreases with postnatal development and restricts plasticity in the visual cortex [Putignano et al., 2007]. HDACs have also been shown to modulate hippocampal LTP and memory [Levenson et al., 2004], predominantly by the specific regulation of CREB-dependent transcriptional activation [Vecsey et al., 2007]. In addition, it was observed that reducing HDAC activity could counteract neuronal degeneration and recover learning and memory in a mouse model of neurodegenerative disease [Fischer et al., 2007]. Upregulation of HDAC4 may thus limit plasticity and increase neurodegeneration in diseases of the CNS that are associated with increased levels of Notch1 expression.

Taken together, this study uncovers a negative feedback mechanism that restricts Notch1-signalling in the neocortical pyramidal cells and identifies potential new target genes of Notch1 mediated transcription that may be involved in regulating neurite growth and cortical plasticity. This may prove to be a useful resource for future studies aiming to uncover how Notch1-signals affect the developing and adult CNS.

Acknowledgements

We thank Matthew Bence, Sarra Riahi and Simone van Soest for technical assistance and Susumu Tonegawa and Kazu Nakazawa for supplying the G35-3-Cre mice.

References

Barnes AP, Lilley BN, Pan YA, Plummer LJ, Powell AW, Raines AN, Sanes JR, Polleux F. LKB1 and SAD kinases define a pathway required for the polarization of cortical neurons. Cell 2007; 129: 549-563.

Berezovska O, Jack C, Deng A, Gastineau N, Rebeck GW, Hyman BT. Notch1 and amyloid precursor protein are competitive substrates for presenilin1-dependent gamma-secretase cleavage. J Biol Chem 2001; 276: 30018-30023.

Bertos NR, Wang AH, Yang XJ. Class II histone deacetylases: structure, function, and regulation. Biochem Cell Biol 2001; 79: 243-252.

Boom A, Pochet R, Authelet M, Pradier L, Borghgraef P, Van Leuven F, Heizmann CW, Brion JP. Astrocytic calcium/zinc binding protein S100A6 over expression in Alzheimer's disease and in PS1/APP transgenic mice models. Biochim Biophys Acta 2004; 1742: 161-168.

Bray SJ. Notch signalling: a simple pathway becomes complex. Nat Rev Mol Cell Biol 2006; 7: 678-689.

Dahlhaus M, Hermans JM, Van Woerden LH, Saiepour MH, Nakazawa K, Mansvelder HD, Heimel JA, Levelt CN. Notch1 signalling in pyramidal neurons regulates synaptic connectivity and experience-dependent modifications of acuity in the visual cortex. J Neurosci 2008; 28: 10794-10802.

de Strooper B, Annaert W, Cupers P, Saftig P, Craessaerts K, Mumm JS, Schroeter EH, Schrijvers V, Wolfe MS, Ray WJ, Goate A, Kopan R. A presenilin-1-dependent gamma-secretase-like protease mediates release of Notch intracellular domain. Nature 1999; 398: 518-522.

Ermekova KS, Zambrano N, Linn H, Minopoli G, Gertler F, Russo T, Sudol M. The WW domain of neural protein FE65 interacts with proline-rich motifs in Mena, the mammalian homolog of Drosophila enabled. J Biol Chem 1997; 272: 32869-32877.

Fischer A, Sananbenesi F, Wang X, Dobbin M, Tsai LH. Recovery of learning and memory is associated with chromatin remodelling. Nature 2007; 447: 178-182.

Fischer DF, van Dijk R, Sluijs JA, Nair SM, Racchi M, Levelt CN, van Leeuwen FW, Hol EM. Activation of the Notch pathway in Down syndrome: cross-talk of Notch and APP. FASEB J 2005; 19: 1451-1458.

Hasson P, Egoz N, Winkler C, Volohonsky G, Jia S, Dinur T, Volk T, Courey AJ, Paroush Z. EGFR signalling attenuates Groucho-dependent repression to antagonize Notch transcriptional output. Nat Genet 2005; 37: 101-105.

Inoue E, Mochida S, Takagi H, Higa S, guchi-Tawarada M, Takao-Rikitsu E, Inoue M, Yao I, Takeuchi K, Kitajima I, Setou M, Ohtsuka T, Takai Y. SAD: a presynaptic kinase associated with synaptic vesicles and the active zone cytomatrix that regulates neurotransmitter release. Neuron 2006; 50: 261-275.

Jarriault S, Brou C, Logeat F, Schroeter EH, Kopan R, Israel A. Signalling downstream of activated mammalian Notch. Nature 1995; 377: 355-358.

Jenzora A, Behrendt B, Small JV, Wehland J, Stradal TE. PREL1 provides a link from Ras signalling to the actin cytoskeleton via Ena/VASP proteins. FEBS Lett 2005; 579: 455-463.

Kao HY, Ordentlich P, Koyano-Nakagawa N, Tang Z, Downes M, Kintner CR, Evans RM, Kadesch T. A histone deacetylase corepressor complex regulates the Notch signal transduction pathway. Genes Dev 1998; 12: 2269-2277.

Katz WS, Hill RJ, Clandinin TR, Sternberg PW. Different levels of the C. elegans growth factor LIN-3 promote distinct vulval precursor fates. Cell 1995; 82: 297-307.

Kawamura A, Koshida S, Hijikata H, Sakaguchi T, Kondoh H, Takada S. Zebrafish hairy/enhancer of split protein links FGF signalling to cyclic gene expression in the periodic segmentation of somites. Genes Dev 2005; 19: 1156-1161.

Kawase T, Ohki R, Shibata T, Tsutsumi S, Kamimura N, Inazawa J, Ohta T, Ichikawa H, Aburatani H, Tashiro F, Taya Y. PH domain-only protein PHLDA3 is a p53-regulated repressor of Akt. Cell 2009; 136: 535-550.

Kishi M, Pan YA, Crump JG, Sanes JR. Mammalian SAD kinases are required for neuronal polarization. Science 2005; 307: 929-932.

Lafuente EM, van Puijenbroek AA, Krause M, Carman CV, Freeman GJ, Berezovskaya A, Constantine E, Springer TA, Gertler FB, Boussiotis VA. RIAM, an Ena/VASP and Profilin ligand, interacts with Rap1-GTP and mediates Rap1-induced adhesion. Dev Cell 2004; 7: 585-595.

Lai EC. Keeping a good pathway down: transcriptional repression of Notch pathway target genes by CSL proteins. EMBO Rep 2002; 3: 840-845.

Lee HS, Lim CJ, Puzon-McLaughlin W, Shattil SJ, Ginsberg MH. RIAM activates integrins by linking talin to ras GTPase membrane-targeting sequences. J Biol Chem 2009; 284: 5119-5127.

Levenson JM, O'Riordan KJ, Brown KD, Trinh MA, Molfese DL, Sweatt JD. Regulation of histone acetylation during memory formation in the hippocampus. J Biol Chem 2004; 279: 40545-40559.

Lleo A, Berezovska O, Ramdya P, Fukumoto H, Raju S, Shah T, Hyman BT. Notch1 competes with the amyloid precursor protein for gamma -secretase and down-regulates presenilin-1 gene expression. J Biol Chem 2003;

Lu FM, Lux SE. Constitutively active human Notch1 binds to the transcription factor CBF1 and stimulates transcription through a promoter containing a CBF1-responsive element. Proc Natl Acad Sci U S A 1996; 93: 5663-5667.

Oswald F, Winkler M, Cao Y, Astrahantseff K, Bourteele S, Knochel W, Borggrefe T. RBP-Jkappa/SHARP recruits CtIP/CtBP corepressors to silence Notch target genes. Mol Cell Biol 2005; 25: 10379-10390.

Putignano E, Lonetti G, Cancedda L, Ratto G, Costa M, Maffei L, Pizzorusso T. Developmental downregulation of histone posttranslational modifications regulates visual cortical plasticity. Neuron 2007; 53: 747-759.

Raaben M, Groot Koerkamp MJ, Rottier PJ, de Haan CA. Mouse hepatitis coronavirus replication induces host translational shutoff and mRNA decay, with concomitant formation of stress granules and processing bodies. Cell Microbiol 2007; 9: 2218-2229.

Redmond L, Oh SR, Hicks C, Weinmaster G, Ghosh A. Nuclear Notch1 signalling and the regulation of dendritic development. Nat Neurosci 2000; 3: 30-40.

Roepman P, Wessels LF, Kettelarij N, Kemmeren P, Miles AJ, Lijnzaad P, Tilanus MG, Koole R, Hordijk GJ, van d, V, Reinders MJ, Slootweg PJ, Holstege FC. An expression profile for diagnosis of lymph node metastases from primary head and neck squamous cell carcinomas. Nat Genet 2005; 37: 182-186.

Roncarati R, Sestan N, Scheinfeld MH, Berechid BE, Lopez PA, Meucci O, McGlade JC, Rakic P, D'Adamio L. The gamma-secretase-generated intracellular domain of beta-amyloid precursor protein binds Numb and inhibits Notch signalling. Proc Natl Acad Sci U S A 2002; 99: 7102-7107.

Ronchini C, Capobianco AJ. Induction of cyclin D1 transcription and CDK2 activity by Notch(ic): implication for cell cycle disruption in transformation by Notch(ic). Mol Cell Biol 2001; 21: 5925-5934.

Sawtell NB, Frenkel MY, Philpot BD, Nakazawa K, Tonegawa S, Bear MF. NMDA Receptor-Dependent Ocular Dominance Plasticity in Adult Visual Cortex. Neuron 2003; 38: 977-985.

Sestan N, Artavanis-Tsakonas S, Rakic P. Contact-dependent inhibition of cortical neurite growth mediated by notch signalling. Science 1999; 286: 741-746.

Vandesompele J, De Preter K, Pattyn F, Poppe B, Van Roy N, De Paepe A, Speleman F. Accurate normalization of real-time quantitative RT-PCR data by geometric averaging of multiple internal control genes. Genome Biol 2002; 3: RESEARCH0034.

Vecsey CG, Hawk JD, Lattal KM, Stein JM, Fabian SA, Attner MA, Cabrera SM, McDonough CB, Brindle PK, Abel T, Wood MA. Histone deacetylase inhibitors enhance memory and synaptic plasticity via CREB:CBP-dependent transcriptional activation. J Neurosci 2007; 27: 6128-6140.

Wang Y, Chan SL, Miele L, Yao PJ, Mackes J, Ingram DK, Mattson MP, Furukawa K. Involvement of Notch signalling in hippocampal synaptic plasticity. Proc Natl Acad Sci U S A 2004; 101: 9458-9462.

Yang YH, Dudoit S, Luu P, Lin DM, Peng V, Ngai J, Speed TP. Normalization for cDNA microarray data: a robust composite method addressing single and multiple slide systematic variation. Nucleic Acids Res 2002; 30: e15.

Yoo AS, Bais C, Greenwald I. Crosstalk between the EGFR and LIN-12/Notch pathways in C. elegans vulval development. Science 2004; 303: 663-666.

Zhang CL, McKinsey TA, Lu JR, Olson EN. Association of COOH-terminal-binding protein (CtBP) and MEF2-interacting transcription repressor (MITR) contributes to transcriptional repression of the MEF2 transcription factor. J Biol Chem 2001; 276: 35-39.